A Novel Enhancement of Nano Structure by Organic Acid Dopants in Emulsion Polymerization of Poly(*o*-toluidine)

VASANT V. CHABUKSWAR[1]*, AMIT S. HORNE[1], SANJAY V. BHAVSAR[1], KALPANA N. HANDORE[1], PRAKASH K. CHHATTISE[1], SUDAM S. PANDULE[1], DIPAK T. WALUNJ[1], SURESH U. SHISODIA[2], ATTILIO CITTERIO[2], SABRINA DALLAVALLE[3], KAKASAHEB C. MOHITE[4], and VISHWAS B. GAIKWAD[5]

[1]*Department of Chemistry, Nowrosjee Wadia College, University of Pune, Bundgarden Road, Pune- 411001, India*
[2]*Department of Chemistry, Material and Chemical Engineering,"Giulio Natta", Politecnico di Milano, Via Mancinelli 7, 20131 Milano, Italy*
[3]*Department of Food, Environmental and Nutritional Sciences, Università degli Studi di Milano, Italy*
[4]*School of Energy Studies, Department of Physics, University of Pune, India*
[5]*K.T.H.M. College, Nashik, India*

Received September 2013, Accepted November 2013

1 Introduction

The field of conducting polymers has been under intensive research and development because of their interesting and useful properties similar to those of metals, while retaining the processability of conventional polymers. In recent years, polyanilines (PANI) have attracted considerable attention of researchers because of their redox properties and environmental stability along with many other practical applications, such as energy storage, analytical sensors, electrostatic discharge protection, optoelectronic devices, sensors, light emitting diodes, light weight batteries, anti-corrosion paints and antistatic films (1–3). Recent developments have shown that conjugated polymer PANI can also be used in the field of construction of electronic devices, photovoltaic cells sensor, actuator and printed circuit display (4–7). PANI doped with mineral or organic acids shows moderate conductivity. Doping processes tune the properties of conducting polymer from insulator to metallic conductor. However, limited solubility in common organic solvents and poor processability of such conducting polymer are some of the drawbacks. In order to overcome this problem of solubility we have attempted the use of substitutents and functional organic acid as dopant. Considerable interest has been focused on the oxidative chemical polymerization. Various researchers have synthesized nanostructure PANI nano particles, fibers, nano-rods, wires. At present, different oxidative chemical methods have been used to produce variety of products, such as template methods,

*Address correspondence to: Vasant V. Chabukswar Department of Chemistry, Nowrosjee Wadia College, University of Pune, Bund garden Road, Pune- 411001, India. Tel.: +91020 26162944; Fax: +9102026162944; E-mail: vvchabukswar@gmail.com

interfacial polymerization, micro emulsion, and seeding polymerization (8). Emulsion polymerization methods have several distinct advantages. It does not depend on the nature, type of template and dopant. Thermal and viscosity restraints of nano structured materials are much less significant than in bulk material. A broad range of organic and inorganic acids can be used as dopants for this method. Emulsion polymerization can be accomplished in one pot with a broad range of solvent pairs. An emulsion polymerization was studied by adding structural directing molecules such as polyelectrolyte, templates and surfactants to obtain polymer nanostructure (9, 10). It also avoids the use of phase transfer reagent. However, all these methods depend on emulsifier species, very complex bulky surfactants, templates and strong inorganic acid as dopants. The removal of inorganic impurities, large bulky template surfactants from the polymer product is difficult. These drawbacks are circumvented by using functional organic acid as dopants and improving the product solubility in common organic solvents.

In the present work we have explored the synthesis of poly(*o*-toluidine) by emulsion polymerization using functional organic acids as dopants (Sch. 1). This method does not depend on the nature of template, the emulsifying agent or phase transfer agent. Use of organic acid provides excellent advantages over strong inorganic acids, which show a detrimental effect on the emulsion polymerization system and polymer structural properties. The effect of the parameters such as concentration of organic dopants, oxidant and solvent, on the polymer properties was investigated and found to be effective to achieve to the formation of nano structures POT.

2 Experimental

2.1 Materials

All chemicals used were of analytical grade, *o*-toluidine, oxalic acid, citric acid, tartaric acid and ammonium persulfate were purchased from Qualigen and Merck. Double distilled de-ionized water was used as a medium for the polymerization reactions.

2.2 Preparation of Poly(*o*-toluidine)

A general procedure for the preparation of poly(*o*-toludine) by emulsion polymerization: At 0–5°C temperature monomer *o*-toluidine (0.1M) was taken in a 100 mL round bottom flask and dissolved in the organic solvent chloroform, to this solution, oxidant ammonium persulfate (0.1M) dissolving in 10 mL of double distilled water and acrylic acid (0.01M) were added. To this resultant reaction mixture aqueous solution of acid as a dopant was added (0.1 M) (such as tartaric acid or citric acid or oxalic acid). The reaction mixture was stirred at 0–5°C, during the reaction the colorless emulsion turned green; the reaction was allowed to proceed for 4 h at 0–5°C. The dark green color solution of poly(*o*-toluidine) in chloroform was dried over anhydrous sodium sulfate and nanoparticles were collected by filtration through nylon 2 μ filter paper from the emulsion. The synthesized poly(*o*-toluidine) was purified by washing with acetone and water. This pure poly (*o*-toluidine) salt was filtered off and dried under vacuum for 48 h.

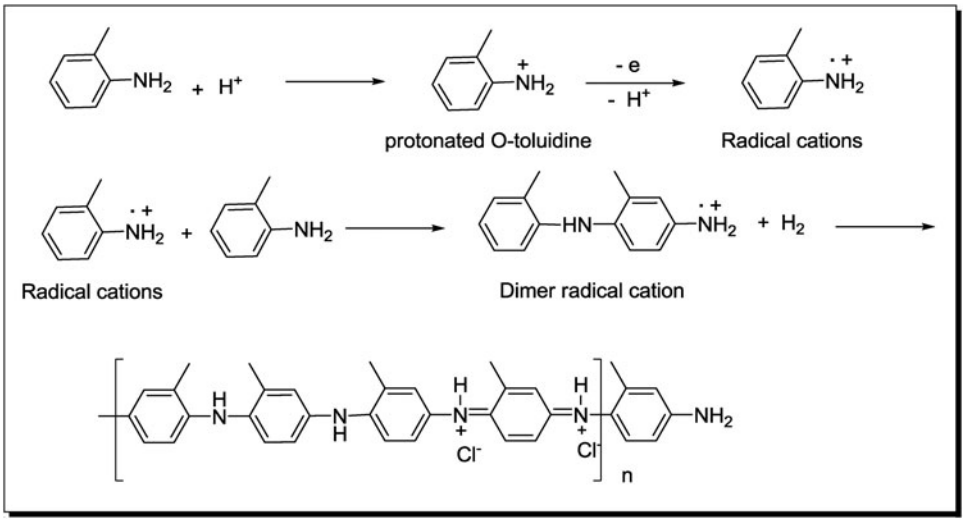

Sch. 1. General mechanism of poly(ortho-toluidine).

2.3 General Reaction Mechanism of Pot Synthesis

Scheme 1 shows the general mechanism of poly(ortho-toluidine).

2.4 Characterization of Polymer

Ultraviolet-visible absorption spectra's of the polymers in *m*-cresol as a solvent were recorded by using λ-200 double beam spectrophotometer (Perkin-Elmer) in the range of 300–1050 nm. The polymer solutions were prepared by dissolving 2 mg POT in 10 mL of *m*-cresol. FTIR measurements were recorded on a Perkin-Elmer 1600A spectrometer (frequency range 400–4000 cm^{-1}). The samples were mixed with KBr and pressed into a pellet (polymer and KBr ratio was 1:150 mg). X-ray diffraction studies were performed on a Bruker AXS D–8 Advance X-ray diffractometer using CuKα radiation source ($\lambda = 1.542$ A°). The spectra were recorded in the range of $2\theta = 0$ to 50° and scanning was performed at rate of 2° min^{-1}. Electrical conductivity of the samples was measured at room temperature by the four-probe method using pressed pellets. The pellets were obtained by subjecting the polymer sample (150 mg) to a pressure of 950 kg cm^{-2}. The material used for XRD analysis was in the pellet form (diameter 12 mm, thickness 3 mm). The polymer samples were characterized with scanning electron microscope (SEM), JEOL-JSM-6360 A.

3 Results and Discussion

3.1 UV Visible Spectral Analysis

The optical absorption spectra's of tartaric acid doped polyaniline and POT polymers doped with various organic acids in *m*-cresol are shown in Figure 1. It can be clearly seen that all compounds shown three major characteristic absorption peaks at about ~380 nm, ~490 nm and broad peak at ~710–820 nm. The band appeared at ~340 nm could be assigned to the π-π^* transition of the benzenoid rings which relates to the extent of conjugation between adjacent aromatic phenyl rings in the polymeric chain (11). The broadband at ~490 nm and ~710–820 nm appeared to be due to the electron transfer from the valence band to the polaron-bipolaron level (12–14). The appearance of these bands confirmed the characteristic conducting phase of the polymer. The intensity of the peaks at ~490 nm and 820 nm was observed to be higher in tartaric acid doped POT compared with oxalic acid and citric acid doped POT. Absorption peaks of citric acid shown a red-shift at ~375 nm and ~420 nm, indicating low energy needed for π-π^* transition. It is attributed to the strengthened interaction between tartaric acid and the polymer back bone. These peaks are well developed in TA doped polyaniline. The peak gradually shifted towards lower wavelength in case of POT, doped with organic acid. These shifts of the two absorption peaks are exhibited in POT samples, implying a decrease in the extent π- conjugation. Kim et al., have proposed that, this was due to induction and steric effect of the substituent (CH_3-group), which are occupied a dominant position and interface between the chains, therefore the effective conjugation length were decrease in organic acid doped poly(*o*-toluidine) (15). These results also suggest that the absorption in the electronic absorption spectra depend on the nature and concentration of functional dopant, polymer-solvent interaction, and nature of the solvent.

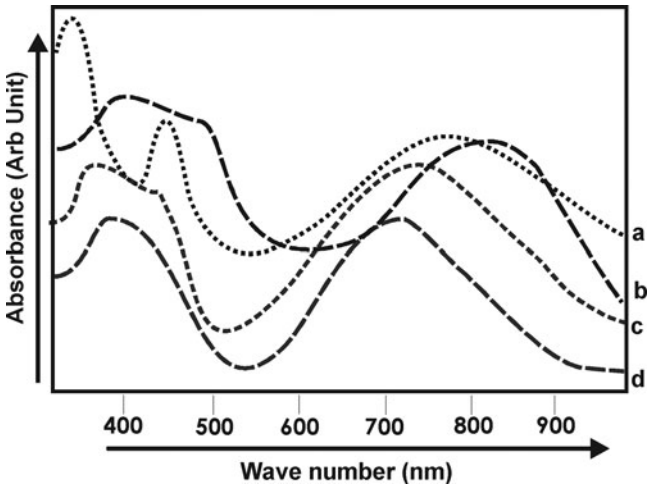

Fig. 1. UV-VIS absorption spectrum's of polymers in *m*-cresol as a solvent (**a**)Polyaniline/ Tartaric acid, (**b**) POT/Tartaric acid, (**c**) POT/Oxalic acid, (**d**) POT/Citric acid.

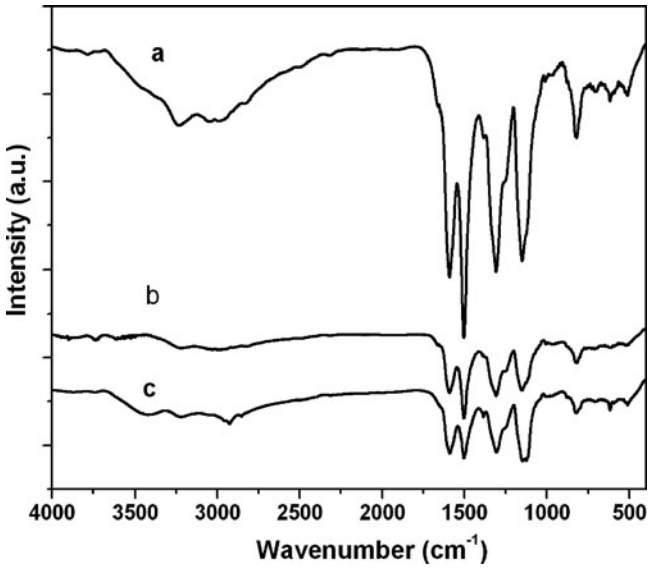

Fig. 2. FTIR spectra of POT doped with different acids (**a**) POT/TA, (**b**) POT/OA, (**c**) POT/CA.

Table 1. Selected FTIR bands (cm^{-1}) of poly(*o*-toluidine) doped with different organic acids

POT/TA	*POT/OA*	*POT/CA*	*Peaks Assignment*
broad peak 3400–3100	broad peak 3400–3100	broad peak 3400–3100	The broad peak accounts for the degree of protonation
1586	1596	1567	C=C stretching vibration of aromatic ring
1496	1497	1502	C−N stretching of the secondary aromatic amine
1306	1313	1305	C−N stretching mode
1151	1160	1142	C−H bending (In plane)
828	819	825	Para coupling
707	710	716	C−H bending vibration (out of plane)

3.2 FTIR Spectral Analysis

FTIR spectroscopy was used to confirm the structure of the polymers obtained by the emulsion polymerization method. The FTIR spectrums of the POT doped with different acids such as (a) tartaric acid, (b) oxalic acid, and (c) citric acid are shown in Figure 2 and peak values for functional groups assigned are given in Table 1 The spectral peaks of all the organic acid doped samples are similar to each other, indicating the chemical structure of the polymer backbone are the same. The characteristic bands in the FTIR spectrum of organic acid doped POT occurred at 2810, 1586, 1496, 1313, 1261, 1160 and 716 cm^{-1} confirmed the POT polymer structure. The broad band at ∼3400–3100 cm^{-1} is assigned to the asymmetric NH_2^+ stretching modes. The symmetric NH_2^+ stretching may overlap with the asymmetric NH_2 stretching mode, as observed in broadness of peak at∼3400–3100 cm^{-1}. In additional two broad peaks at 3000 and 1360–1370 cm^{-1} attributed to a C−H stretching vibration of CH_3 group. A strong absorption band at ∼1100–1160 cm^{-1} was related to an aromatic C−N stretching vibration. Furthermore, the peaks at 820–840 and 760–800 cm^{-1} were assigned to 1,2,4/trisubstituted benzene ring (16).

3.3 Scanning Electron Microscopy Analysis

The morphology of the organic acid doped POT can be imaged using electron microscopy. As can be seen from Figure 3, tartaric acid doped POT particles are in the form of uniform rod shaped nano fibers with diameter of 20–50 nm. While POT doped with oxalic and citric acid shows uniform spherical nano-grains shaped particles with an average diameter of 50–80 nm. The morphology of citric acid doped POT is spherically shaped with comparatively smoother particle surface and highly aggregated. A comparison indicated that TA doped POT had remarkably different morphology. These differences may be explained by considering the interaction between organic functional dopants and charged ionic polymer chain. Among these tartaric acid increase the polymer chain interaction more intense than oxalic and citric acid, leads to extra doping. This indicates that morphology, conductivity of polymer is influenced by the dopant and method of synthesis used (17). It is interesting to note that the diameter of nanoparticles or fibers are affected by the dopants used in the polymerization as shown in Figure 3. It was observed that the traditional aqueous chemical polymerization using common mineral acids such as HCl, H_2SO_4 and $HClO_4$ yields granular morphology of polymer. The granular shape is related to the heterogeneous nucleation mechanism of polymerization. This difference may be explained by the interaction between dopant and polymer chain. Recent work has shown that the use of template, functional dopants control the morphology, shape and size of the nanoparticles (18–19). It is observed that acrylic acid not only functions as an effective dopant but also as a template guiding the polymer chain conformation by forming micelle centers during polymer growth (20). Morphology of POT doped with oxalic, tartaric, and citric acid may be different depending on their different molecular structure, it is observed that such functional organic acids act as dopant and soft template that guide the formation of polymer nanostructure (21).

Table 2. Comparative electrical conductivity of POT doped with different organic acids

No	*Polymer*	*Conductivity S cm^{-1}*
a	POT/TA	2.2×10^{-1}
b	POT/OA	8.3×10^{-2}
c	POT/CA	4.5×10^{-4}
d	PANI/TA	2.4×10^{-2}

3.4 X-Ray Diffraction Studies of Pot Synthesized

The XRD pattern of the POT doped with different acids such as tartaric, citric, oxalic acid are shown in Figure 4. The XRD patterns of organic acids doped POT shows three typical diffraction peaks at $2\theta = 9$, 18–20° and ∼25°. The peaks at $2\theta = 20°$, which is common in all cases, can be assigned to the periodic distance between the organic dopants and nitrogen atom of the adjacent benzenoid ring

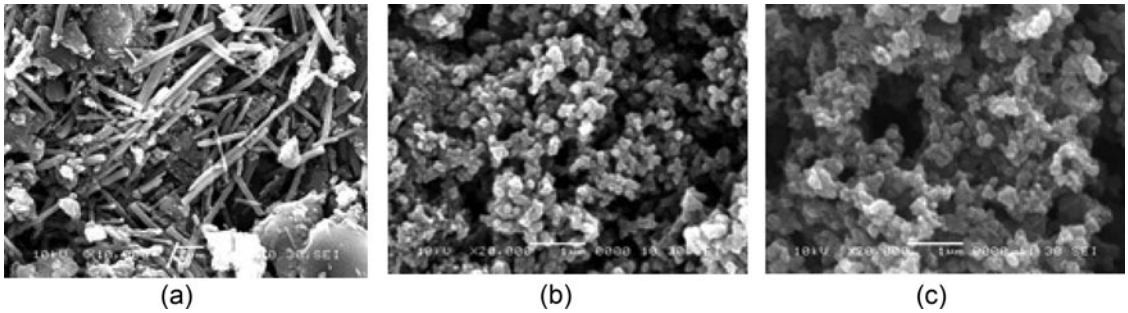

Fig. 3. SEM images of poly(*o*-toluidine) doped with different acids: **(a)** POT/TA, **(b)** POT/OA, **(c)** POT/CA.

of the polymer chain. This result reveals that well organized; morphology can be found by emulsion polymerization method using organic acids. The Bragg diffraction peak of the POT polymer powder exhibits $2\theta = 26^\circ$ indicating the relatively good polyaniline sub chain alignment since the diffraction at $2\theta \sim 25$ to 26° is a characteristic peak of the partial crystalline nature of POT. These peaks indicate that the resultant polymers are in the doped emeraldine salt form. Furthermore, this result suggests that the higher conductivities of the POT doped with TA come from the better ordered chain conformation, as well as the nanorod shaped morphology result into higher doping level (22–24).

3.5 Electrical Conductivity Study of POT

The electrical conductivity of POT doped with different organic acids were studied and found that it depends on the nature, type of functional organic dopant, oxidation state, particle morphology, crystallinity etc. The electrical conductivity of POT doped with tartaric acid was higher than that of citric and oxalic acid doped POT. It was observed that the conductivity of POT polymer increases with increasing doping degree, crystallinity and the higher relative intensity of quinoid to benzenoid ring mode. It was found that the fibrilar morphology of POT/TA has an enhanced effect on the conductivity. A decrease in diameter of nanofibers of TA doped POT may lead to enhanced doping, higher degree and well organized crystallinity and higher conductivity. The conductivity of POT salt was decreased with increase in number of −OH and −COOH groups in carboxylic acid which has affected the morphology of POT (25–27).

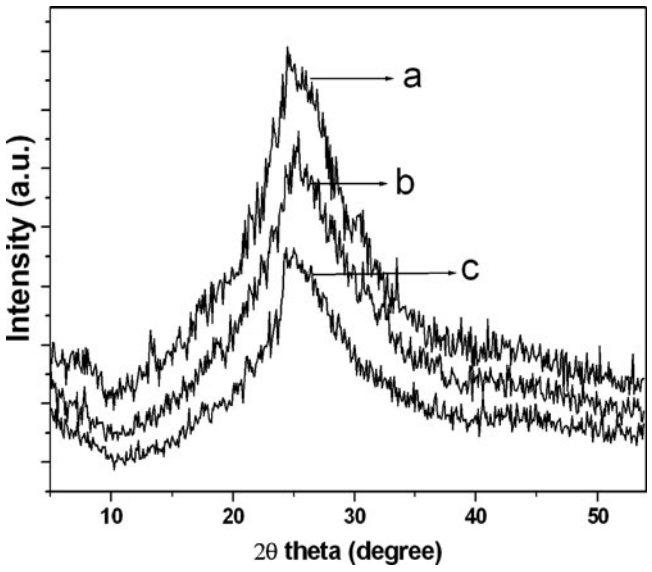

Fig. 4. XRD spectrums of poly (*o*-toluidine) doped with different acids (**a**) POT/TA, (**b**) POT/OA, (**c**) POT/CA.

4 Conclusions

Poly(*o*-toluidine) nano-particles were prepared by novel emulsion polymerization method using organic acids as dopant, without any hard template. The synthetic conditions are very facile and can be worked out with a broad range of organic acid dopants, monomer concentration. Emulsion polymerization can be effectively used as a morphology selective synthesis, easy method to prepare highly oriented nano structures of POT. It was found that the use of organic dopants, monomer concentration have characteristic effect on the physico-chemical properties of polymer. The POT synthesized by using oxalic, and citric acid dopant has granular morphology, moderate conductivity and crystallinity. POT nanoparticles prepared with tartaric acid dopant showed average particle size of 50–70 nm with uniform fibrilar morphology. The average diameter increases from 20 to 80 nm as dopant varies from citric acid to oxalic acid doped POT. Comparative study indicated that among these organic acids, POT doped with tartaric acid, shows fibrilar morphology better crystallinity and conductivity. These results indicated that polymer size, morphology, physico-chemical properties depends on size and nature of functional dopants. A decrease in particle size resulted into more effective structural order, hence, better crystallinity and enhanced conductivity.

Acknowledgements

The authors gratefully acknowledge C-MET, NCL and Nowrosjee Wadia College for providing general facilities for this work.

Funding

The authors gratefully acknowledge the financial support provided by UGC, New Delhi, and ISRO-University of Pune.

References

1. Lee, K., Cho, S., Park, S., Heeger, A., Lee, C., Lee, S. (2006) Nature, 65, 441.
2. Lee, K., Heeger, A. (2002) Synth. Metals, 128, 279.
3. Mamoru, N., Hidetak,T., Kiyoshi, S. (2005) Adv. Polym. Sci., 175, 1.
4. Huang, Li., Kaner, R. (2009) Acc. Chem. Res., 42, 135.
5. Cuentas Gallegos, A., Lira Cantù, M., Casanpastor, N., Gomez Romero, P. (2005) Adv. Funct. Mater., 15, 1125.
6. Chern, C. S. (2006) Prog. Polym. Sci., 31, 443.
7. Chen, Z., Xu, L., Li, W., Waje, M., Yan, Y. (2006) Nanotechnology 17, 5254.
8. Gan, L., Chew, C., Chan. S., Ma, L. (1993) Polym. Bull., 31, 347.
9. Palaniappan, S., Nivasu,V. (2002) New J. Chem., 26, 1490.
10. Jin, J., Iyoda, T., Cao, C., Sang, Y., Jiang, L., Zhu, D. (2001) Angew. Chem. Int. Ed., 40, 2135.
11. Chabukswar, V., Athawale, A. (2002) Mater. Chem. Phys., 73,106.
12. Wan, M. (2008) Adv. Mater., 20, 2926.
13. Wan, M. (1989) Synth Metals, 31, 51.
14. Tzou, K., Gregory, R. (1993) Synth. Metals, 53, 365.
15. Kim, Y., Chiang, J., Heroger, A. (1989) Synth. Metals, 29, 285.
16. Wan, M., Yang, J. (1995) J. App. Poly. Sci., 55, 339.
17. Hesheng, X., Wang, Qi. (2001) J. Nanopart. Res., 3, 401.
18. Tran, H., Kaner, R. (2006) Chem. Commum., 3915.
19. Xin, W., Wei, W., Jian, F., Yi-bo, Z. (2011) Ind. Eng. Chem. Res., 50, 5589.
20. Palle, S.R., Sathyanarayana, D.N., Palaniappan, S. (2002) Macromolecules, 35, 4988.
21. Chabukswar, V., Bhavsar, S., Mohite, K. (2012) J. Macromol. Sci., Part A: Pure Appl. Chem., 49, 547.
22. Wei, Z., Zhang, L., Yu, M., Wan, M. (2003) Adv. Mater., 15, 1382.
23. Jiaxing, H., Kaner, R. (2004) J. Am. Chem. Soc., 126,851.
24. Du, X., Zhou, C., Mai, Y. (2008) J. Phys. Chem., 112, 198.
25. Li, Q., Cruz, L., Phillips, P. (1993) Mater. Phys., 47, 1840.
26. Dan, L., Kaner, R. (2006) J. Am. Chem. Soc., 128, 968.
27. Chabukswar, V., Bhavsar, S. (2010) Chem. Chem. Technol., 4, 277.
28. Chabukswar, V., Bhavsar, S., Horne, A. (2011) Chem. Chem. Technol., 5, 37.
29. Chabukswar, V., Horne, A., Bhavsar, S. (2012) J. Macromol. Sci., Part A: Pure Appl. Chem., 49, 926.